SRL-0096-TR

AR-006-969

DEPARTMENT OF DEFENCE

DEFENCE SCIENCE AND TECHNOLOGY ORGANISATION

SURVEILLANCE RESEARCH LABORATORY

SALISBURY, SOUTH AUSTRALIA

TECHNICAL REPORT

SRL-0096-TR

MODIFIED GRAM-SCHMIDT ALGORITHM FOR ADAPTIVE SIDELOBE CANCELLATION

M. STONE
(Ericsson Defence Systems)

APPROVED FOR PUBLIC RELEASE

MARCH 1992

AR-006-969

DEPARTMENT OF DEFENCE

DEFENCE SCIENCE AND TECHNOLOGY ORGANISATION

SURVEILLANCE RESEARCH LABORATORY

SALISBURY SOUTH AUSTRALIA

TECHNICAL REPORT

SRL-0096-TR

MODIFIED GRAM-SCHMIDT ALGORITHM FOR ADAPTIVE SIDELOBE CANCELLATION

M. STONE
(Ericsson Defence Systems)

SUMMARY

This report assesses the performance of an adaptive sidelobe cancellation system based on the Modified Gram-Schmidt algorithm. A large phased array antenna has been modelled utilising this adaptive sidelobe cancellation technique and relevant scenarios simulated. In order to reduce antenna pattern degradation, noise injection has also been implemented.

POSTAL ADDRESS: Director, Surveillance Research Laboratory,
PO Box 1500, Salisbury, South Australia 5108

Contents

Figures

Appendices

1 SCOPE

This report discusses a study into Adaptive Sidelobe Cancelling (ASLC) techniques. A large phased array antenna has been simulated in order to judge the effectiveness of ASLC against noise jamming and to assess the performance of several algorithms, in particular, the modified Gram-Schmidt algorithm.

Initially, the Modified Gram-Schmidt (MGS) algorithm was compared with the Direct Matrix Inversion (DMI) algorithm to ascertain what advantages, if any, the MGS algorithm has over DMI. The MGS algorithm was then developed further in an attempt to reduce the antenna pattern degradation due to excess degrees of freedom normally associated with ASLC implementation.

Section 2 provides a background to the theory associated with adaptive sidelobe cancellation. The methodology behind the DMI and MGS algorithms is discussed as well as some of the broader areas of ASLC that need consideration such as transient sidelobe levels, mainlobe degradation, eigenvalues and the theory behind successful reduction of transient sidelobe levels due to excess degrees of freedom.

Section 3 details the assumptions and simplifications inherent in the model of the large phased array used in the study of ASLC. The most significant component of this discussion involves the jammers and the corresponding jammer signals received by the array. The section concludes with comparisons between a realistic radar system and the simplifications in this model in terms of the antenna elements and the receiver hardware.

Section 4 reviews some of the significant results obtained from the model, concentrating initially on the similarities between DMI and MGS and then highlighting the scenarios where MGS improves on the results obtained by DMI. Results that allow comparisons of transient sidelobe levels and mainlobe degradation due to excess degrees of freedom are then presented in order to complement the theoretical discussion of the subject presented in section 2. Techniques to reduce these problems have been implemented and the results provided by the improved models are compared to previous results.

Section 5 summarises the results provided in section 4 and makes several recommendations regarding a successful implementation of ASLC into a real system. This discussion highlights the need for situation dependent ASLC in which important parameters must be adjusted in order to maximise performance for a given scenario.

2 THEORY

2.1 Adaptive Sidelobe Cancelling

Adaptive sidelobe cancelling, for the purposes of this discussion, is defined as adapting the antenna array sidelobes in order to place nulls in the directions of point noise interference sources. The architecture required to achieve this is shown in figure 2-1.

Referring to this diagram, the main channel represents the sum of the signals from all the elements in the array and may be thought of as the system before the introduction of ASLC. The auxiliary elements may be elements in the main array (*element re-use*) or elements separate from the main array. The fact that a subset of auxiliary elements is used to adapt the antenna pattern as opposed to applying adaptive weights to all the elements in the main channel means the system is a *partially adaptive array* instead of a *fully adaptive array*.

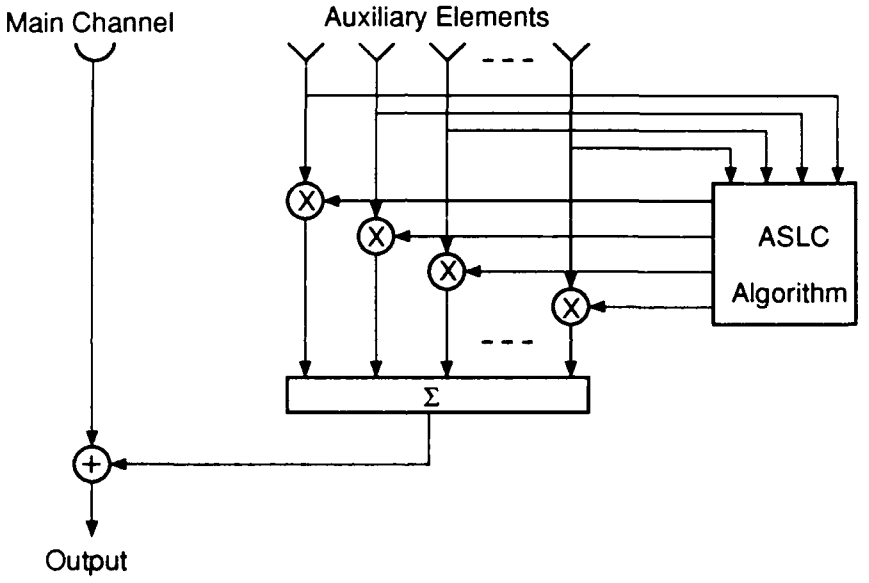

Figure 2-1 Adaptive Sidelobe Cancelling System.

Adaptation of the sidelobe pattern is achieved by weighting the signals obtained from the auxiliary elements in such a way that once added to the main channel, nulls appear in the sidelobes in the directions of the interfering noise sources. The complex weights applied to auxiliary elements are generally calculated by an ASLC algorithm that attempts to maximise the signal to noise ratio of the main channel.

Applebaum [1] has derived an expression for the weights in a fully adaptive array i.e. where all elements of the array may be individually weighted.

$$\underline{w}_{opt} = \mu \underline{M}^{-1} \underline{s}^{*}$$

where $\underline{w}_{opt}$ are the optimum weights,

$$\underline{w}_{opt} = \left[w_1, w_2, \cdots, w_N\right]^T$$

$\underline{M}$ is the covariance matrix of the element signals (the asterisk represents complex conjugation)

$$\underline{M} = [m_{ij}] \, , \; m_{ij} = E\{x_i^* x_j\}$$

$\underline{s}$ is a steering vector describing the complex phase relationship between the antenna elements

$$\underline{s} = \left[s_k\right] \, , \; s_k = exp\left(j\frac{2\pi kd}{\lambda}\sin\theta\right)$$

and μ is a scaling factor influencing convergence but not the SNR performance. This equation is known as the Weiner-Hopf equation.

For the purposes of this model, only a partially adaptive array will be considered where a subset of the array elements is weighted and used to perform the sidelobe cancelling.

Yuen [2] has adapted the equation derived by Applebaum to reflect a partially adaptive array.

$$\underline{w}_{opt} = \underline{M}^{-1}\underline{c}^*$$

where again $\underline{w}_{opt}$ are the optimum weights, $\underline{M}$ is the covariance matrix of the auxiliary element signals, and $\underline{c}$ is the vector representing cross-correlation between the auxiliary element signals x_i and the main channel x_0 (when discussing partially adaptive arrays it is customary to describe the main channel as the 0^{th} auxiliary.)

$$\underline{c} = [c_i] \, , \; c_i = E\{x_i^* x_0\}$$

2.2 Direct Matrix Inversion

There are several way to apply this equation to a real-life radar system. Early work focussed on the *least mean square* (LMS) algorithm developed by Widrow et al [3] in 1967. A series of analog feedback loops attempt to converge to the optimum weights, however, this technique suffers from poor initial convergence and thus poor adaptivity in a time varying environment. The main advantage of the LMS algorithm is its computational simplicity and the fact that it can be implemented using simple analog blocks.

With today's computing power and a general trend towards digital implemention much work has gone into sampling the auxiliary signals and subsequently inverting the covariance matrix $\underline{M}$ and multiplying it with the cross-correlation vector $\underline{c}$; a technique known generally as *direct matrix inversion* (DMI) [4].

Digital processing also enables the use of "*batch*" processing in which the weights are not re-calculated continuously but are processed in batches ; a set of data (corresponding to a predefined period of time) is applied to the algorithm and the weights that are derived are then applied to the data to obtain the suppressed signal.

In order to improve the speed of calculation, a subset of this data may be used to calculate the weights which are then applied to the entire set of data. This is known as *non-concurrent* processing as opposed to *concurrent* processing where the weights are applied to the same data used to obtain the weights.

It is customary to denote the sampled signals as vectors where the dimensionality of the vector is defined by the number of time samples, thus the auxiliary signal for the i^{th} auxiliary channel becomes

$$\underline{x}_i = [x_{i,1}, x_{i,2}, \ldots, x_{i,n}]^T \quad i = 1, 2, \ldots, N$$

and the main signal becomes

$$\underline{x}_0 = [x_{0,1}, x_{0,2}, \ldots, x_{0,n}]^T$$

where n and N represent the number of time samples and the number of auxiliary elements respectively.

The covariance matrix $\underline{\underline{M}}$ may be adapted for the sampled case to

$$\underline{\underline{M}} = [m_{ij}], \; m_{ij} = \frac{1}{n}\sum_{k=1}^{n} x_{i,k}^* x_{j,k}$$

and the cross-correlation vector $\underline{c}$ becomes

$$\underline{c} = [c_i], \; c_i = \frac{1}{n}\sum_{k=1}^{n} x_{i,k}^* x_{0,k}$$

The covariance matrix $\underline{\underline{M}}$ is inverted and multiplied by the cross-correlation vector $\underline{c}$ to provide the weights.

DMI provides a direct solution to the Weiner-Hopf equation, however, since it involves a matrix inversion, problems can arise in computing this inversion if the matrix is ill conditioned. This manifests itself as a sensitivity to round-off errors and the processor performing the inversion requires sufficient accuracy to avoid this problem.

2.3 Covariance Matrix Ill-conditioning

Consider the solution to the Weiner-Hopf equation in which a small error $\underline{\underline{E}}$ is applied to the covariance matrix $\underline{\underline{M}}$. This error is usually due to the finite numerical accuracy inherent to all digital processors. We define the resultant error on the complex weights $\underline{w}$ after inverting the covariance matrix and multiplying it by the cross-correlation vector $\underline{c}$ to be $\underline{e}$.

$$\underline{w} = \underline{\underline{M}}^{-1}\underline{c}$$
$$\underline{W} + \underline{e} = (\underline{\underline{M}} + \underline{\underline{E}})^{-1}\underline{c}$$

It can be shown [7] that

$$\frac{\|\underline{e}\|}{\|\underline{w}\|} \leq \frac{\|\underline{M}^{-1}\| \, \|\underline{M}\| \frac{\|\underline{E}\|}{\|\underline{M}\|}}{1 - \|\underline{M}^{-1}\| \, \|\underline{M}\| \frac{\|\underline{E}\|}{\|\underline{M}\|}}$$

where

$\|\underline{A}\|$ = (maximum eigenvalue of matrix $\underline{A}^{H}\underline{A}$)$^{1/2}$

($\underline{A}^{H}$ represents the conjugate transpose of $\underline{A}$.)

and

$\|\underline{a}\|$ = the magnitude of vector $\underline{a}$

This expression gives the relative error $\|\underline{e}\|/\|\underline{w}\|$ in $\underline{w}$ in terms of the relative error $\|\underline{E}\|/\|\underline{M}\|$ in $\underline{M}$ which allows us to assess how much error is introduced to the complex weights $\underline{w}$ because of the illconditioning of the covariance matrix $\underline{M}$. It can be seen that this error is dependent on the quantity $\|\underline{M}\| \, \|\underline{M}^{-1}\|$.

We call this quantity the *condition number* c of covariance matrix $\underline{M}$.

Recalling our definition of the matrix norm,

$\|\underline{M}\|$ = (maximum eigenvalue of matrix $\underline{M}^{H}\underline{M}$)$^{1/2}$

= (maximum eigenvalue of matrix $\underline{N}$)$^{1/2}$

where $\underline{N} = \underline{M}^{H}\underline{M}$

By definition

$$| \lambda \underline{I} - \underline{N} | = 0$$

where λ are the eigenvalues of $\underline{N}$ and $\underline{I}$ is the identity matrix.

$$| \lambda \underline{N}\underline{N}^{-1} - \underline{N} | = 0$$
$$| -\lambda \underline{N}(\tfrac{1}{\lambda}\underline{I} - \underline{N}^{-1}) | = 0$$
$$| -\lambda \underline{N} | \, | \, (\tfrac{1}{\lambda}\underline{I} - \underline{N}^{-1}) | = 0$$

since $-\lambda\underline{N}$ cannot be equal to 0 for $\underline{N} \neq [0]$ it follows that

$$| \tfrac{1}{\lambda}\underline{I} - \underline{N}^{-1} | = 0$$

Since this is also the definition of the eigenvalues of a matrix, it may be concluded that the eigenvalues of the inverse of the covariance matrix ($\underline{N}^{-1}$) are the inverse of the eigenvalues of the covariance matrix ($\underline{N}$). i.e.

$$\lambda_{\underline{N}} = 1 / \lambda_{\underline{N}^{-1}}$$

Applying this result to our condition number $c = \|\underline{M}\| \, \|\underline{M}^{-1}\|$, it is apparent that $\|\underline{M}^{-1}\|$, the squareroot of the maximum eigenvalue of $\underline{N}^{-1}$, is the squareroot of the inverse of the minimum eigenvalue of $\underline{N}$ and our condition number may now be written

$$c = \sqrt{\frac{\lambda_{max}(\underline{N})}{\lambda_{min}(\underline{N})}}$$

As matrix $\underline{M}$ is symmetric, it follows [8] that

$$\sqrt{\frac{\lambda_{max}(\underline{N})}{\lambda_{min}(\underline{N})}} = \frac{\lambda_{max}(\underline{M})}{\lambda_{min}(\underline{M})}$$

therefore

$$c = \frac{\lambda_{max}(\underline{M})}{\lambda_{min}(\underline{M})}$$

Thus the condition number c of matrix $\underline{M}$ corresponds to the *spread* of the eigenvalues of $\underline{M}$.

The effect that eigenvalue spread has on suppression performance has been investigated to some extent by Monzingo and Miller [9]. For scenarios with an eigenvalue spread below some critical value, DMI is relatively insensitive, however, once the critical value is exceeded, rapid degradation of the jammer suppression results. This critical value of eigenvalue spread at which significant reductions in jammer suppression occur depends largely on the numerical accuracy of the processing system and the size of the covariance matrix i.e. the number of auxiliaries.

It is now apparent that certain covariance matrices used in conjunction with DMI result in errors in the auxiliary weights which leads to poor cancellation and increased sidelobes. The question now arises as to what scenarios would lead to matrix ill-conditioning.

A general eigenvalue evaluation of the covariance matrix in the presence of multiple jammers is well beyond the scope of this document, however, it is generally accepted that the eigenvalues of the covariance matrix tend to reflect the jammer scenario incident on the array [10].

For an N auxiliary system, the covariance matrix will have N eigenvalues. Compton [10] notes that when considering narrow band jammers, these eigenvalues may be divided into two groups ; *significant* eigenvalues ($\lambda_n >> 1$) and *noise* eigenvalues ($\lambda_n \approx 1$). There are as many significant eigenvalues as there are spatially separate interference sources received by the antenna and furthermore, the sum of the eigenvalues is equal to the sum of the signals received by the *auxiliary* channels.

The actual values of the significant eigenvalues varies with jammer direction of arrivals, signal bandwidths and array configuration ; only the sum of the eigenvalues can be predicted.

Considering the equation for the condition number of the covariance matrix, it is apparent that when there are noise eigenvalues (caused by having more auxiliaries that jammers), λ_{min} will be a noise eigenvalue and thus approximately equal to 1. Similarly, as the sum of the eigenvalues is equal to the total stregnth of the interference sources, the value of λ_{max} will be dependent on the total strength of the interference sources.

It may be concluded that covariance matrix ill-conditioning will be most likely to occur when more auxiliaries than necessary are receiving a lot of jammer interference.

If there are no degrees of freedom and hence no noise eigenvalues, it is still possible to have matrix ill-conditioning.

Limiting ourselves to a two jammer, two auxiliary problem, the eigenvalues of the covariance matrix are [5]

$$\lambda_{1,2} = 1 + (P_1 + P_2 \pm [(P_1 - P_2)^2 + 4P_1P_2 \mid \rho \mid^2]^{\frac{1}{2}})$$

where P_1 and P_2 are the jammer powers with respect to the noise level and ρ is the complex correlation coefficient of the auxiliary phasor vectors and is dependent only on jammer directions of arrival and auxiliary position and not the jammer powers.

Assuming that $P_1 > P_2$ and both P_1 and P_2 are real, the condition number of the covariance matrix becomes

$$c = \frac{\lambda_{max}}{\lambda_{min}} = \frac{1+P_1+P_2+\sqrt{(P_1-P_2)^2+4P_1P_2|\rho|^2}}{1+P_1+P_2-\sqrt{(P_1-P_2)^2+4P_1P_2|\rho|^2}}$$

From this it can be seen that as the difference between P_1 and P_2 increases, the condition number c increases which also indicates that with the correct number of auxiliaries for the jammer scenario, matrix ill-conditioning may also occur if the jammers have widely varying power levels.

To remedy the problem discussed above, there are two possible courses of action.

- Increase the numerical accuracy of the processors performing the matrix inversion until the error $\underline{\underline{E}}$ in the covariance matrix results in an insignificant error $\underline{e}$ in the complex weights. This, however, also increases the cost of the system as well as the time required to perform the calculations.
- Utilise an indirect method of inverting the covariance matrix that is insensitive to matrix ill-conditioning.

2.4 Modified Gram-Schmidt

The Weiner-Hopf equation that DMI attempts to solve directly is a least squares estimation of the weights required to provide the maximum signal to noise ratio. Another method for obtaining a solution to this problem is via orthogonalisation algorithms such as the Givens, the Householder and the Modified Gram-Schmidt.

Of these three orthogonalisation techniques, the modified Gram-Schmidt is considered to be the best suited for improving numerical accuracy [6] and as such has been used in this project. The topic of Gram-Schmidt and Modified Gram-Schmidt is discussed further in reference [2].

To apply MGS to adaptive sidelobe cancelling the structure shown in figure 2-2 is required.

It is made up of a lattice of building blocks labelled GS (refer figure 2-3) which perform the individual MGS orthogonalisation of two inputs to produce an output which is subsequently used as input to the MGS building blocks in the next level.

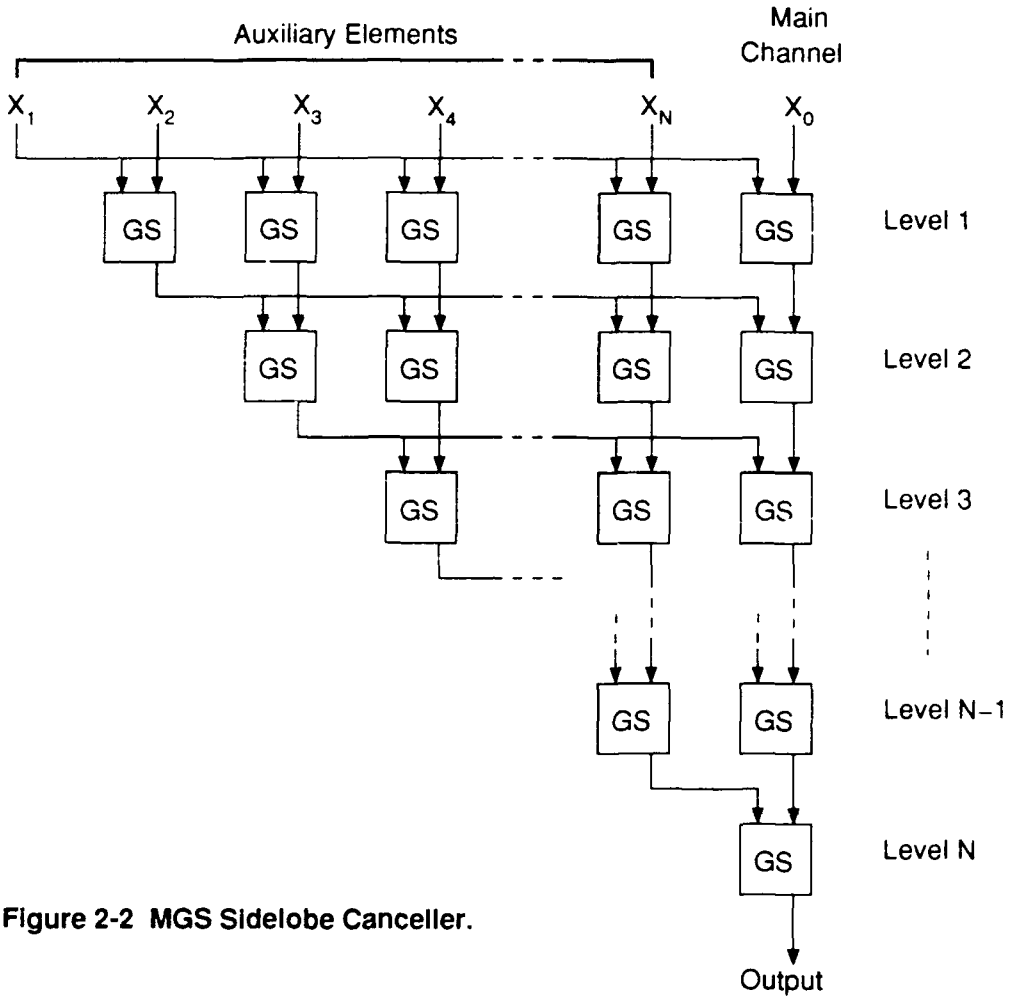

Figure 2-2 MGS Sidelobe Canceller.

In order to understand the operation of the MGS lattice it is necessary to further understand the operation of the MGS building block.

Because of the transient nature of most radar pulses, and their relatively low power relative to a noise jammer, the assumption may be made that the radar return pulse will not affect the ASLC algorithm and as such is ignored.

Therefore the only signals of interest are the jammer signals and the noise.

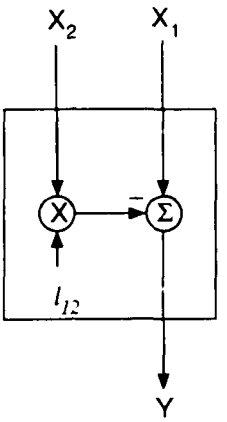

$$l = \frac{\overline{X_1 X_2^*}}{\overline{X_2 X_2^*}}$$

Figure 2-3 GS Processor Unit.

The equation describing the relationship between the two input signals and the output is

$$Y = X_1 - \frac{\overline{X_1 X_2^*}}{\overline{X_2 X_2^*}} X_2$$

This process decorrelates the input X_1 with X_2 ; the result of which is output to Y, which means that when Y and X_2 are cross correlated, the result is 0.

$$\overline{Y X_2^*} = 0$$

For the simple case of X_1 being the main channel and X_2 being an auxiliary element, both in the presence of a single noise jammer, the output Y will be the main channel decorrelated with the auxiliary.

Since the jammer signal is received by the main channel (via the sidelobes) *and* the auxiliary, X_1 and X_2 should be highly correlated. The output Y will therefore be the signal component in X_1 that is uncorrelated with X_2. For this example, Y will be the uncorrelated noise in X_1 as the jammer signal present in the main channel and the auxiliary will be highly correlated.

To expand this simple example to a realistic system, we must introduce more jammers and correspondingly more auxiliaries. In this case the main channel must be decorrelated with all the auxiliaries, hence the triangular structure shown in figure 2-2. Each level of the structure decorrelates one auxiliary with the main channel and all the other auxiliaries ; decorrelation with the other auxiliaries must be performed to prevent signal components already decorrelated being re-introduced back into the main channel when subsequent auxiliaries are decorrelated.

The output of figure 2-2 will be the main channel with the noise jammer signals suppressed, however, as discussed earlier, in order to reduce the time required to perform this cancellation, *non-concurrent* processing may be used ; the system outlined above only achieves sidelobe cancellation *concurrently*.

The system is therefore also required to calculate the complex weights to enable processing similar to that shown in figure 2-1. To obtain these weights, the internal GS weights l_{ij} are retained and the $N+1 \times N+1$ matrix of these internal weights $\underline{L}=[l_{i,j}]+\underline{I}$ is inverted to give the $N+1 \times N+1$ matrix $\underline{T}=[t_{i,j}]+\underline{I}$ where $\underline{I}$ is the identity matrix.

The complex weights w_j make up the bottom row of the matrix $\underline{T}$. i.e.

$$w_j = t_{N+1,j} \quad j = \{1, 2, \ldots, N+1\}$$

for an N auxiliary system. w_{N+1} corresponds to the weight to be applied to the main channel and is equal to 1.

Since only the last row of matrix $\underline{T}$ is required, the following recursive algorithm may be used instead of inverting the entire matrix.

$$t_{N+1,k} = -\sum_{j=k+1}^{N+1} t_{N+1,j}\, l_{j,k}$$

For example, with a 3 auxiliary system (N=3)

$$t_{4,4} = 1$$

$$w_3 = t_{4,3} = -t_{4,4}\, l_{4,3}$$

$$w_2 = t_{4,2} = -t_{4,3}\, l_{3,2} - t_{4,4}\, l_{4,2}$$

$$w_1 = t_{4,1} = -t_{4,2}\, l_{2,1} - t_{4,3}\, l_{3,1} - t_{4,4}\, l_{4,1}$$

It is now a simple matter to apply these weights to the entire set of data.

2.5 Transient Sidelobes

The choice of antenna for radar applications is made on the basis of several important criteria ; high main lobe gain and low sidelobes being two of these. The use of phased array antennas provides some flexibility in antenna pattern design and as will be discussed later, phase and amplitude weighting is generally applied to elements of the array to reduce sidelobes. Unfortunately, the complex weighting of the auxiliary elements tends to reduce the effectiveness of the original weighting which decreases the main lobe response and increases the sidelobes.

The larger the weights, the more effect ASLC has on the original antenna response and hence, the greater increase in sidelobes and degradation of the mainlobe.

There are two main causes of excessively large weights ; one inherent to ASLC systems and the other associated with the shortcomings of real systems.

Consider a one jammer, one auxiliary system where the auxiliary has an isotropic pattern and the complex weight applied to that auxiliary is optimal. In order to cancel the jammer, the complex weight on the auxiliary is set such that the level of the auxiliary is the same as the sidelobe level at the angle of incidence of the jammer.

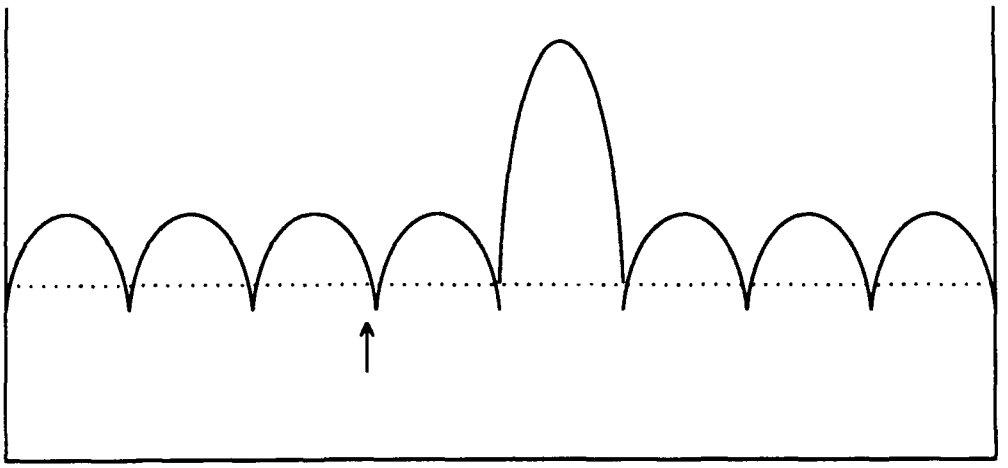

Figure 2-4 Jammer Low on Sidelobes.

Figure 2-4 shows a jammer (indicated by the arrow) incident on the main array (solid line) very low in the sidelobes. The corresponding auxiliary pattern required to cancel this jammer is shown by the dotted line. As the auxiliary pattern (and hence the auxiliary weight) is small compared to the main array pattern, it will have a minimal effect on the overall antenna pattern when subtracted from the main array and hence will not significantly increase the sidelobes or reduce the mainlobe.

The corresponding case for a jammer high on the sidelobes is shown in figure 2-5. As expected the auxiliary pattern is large in comparison to the antenna pattern and when subtracted, excessive sidelobe increases will result. This problem is inherent to ASLC systems.

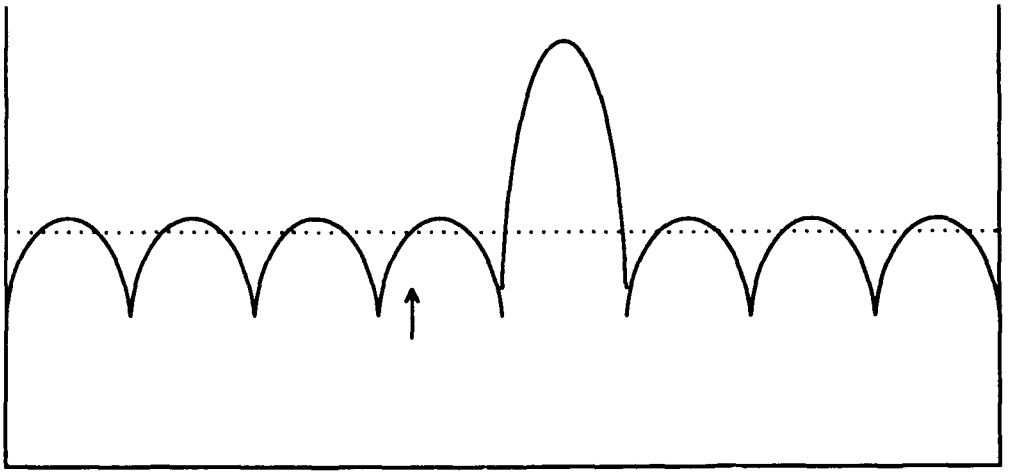

Figure 2-5 Jammer High on Sidelobes.

To reduce the change in antenna response , it is necessary to increase the number of auxiliaries which allows the auxiliary antenna pattern to have a high gain in the direction of the jammer and low gain in all other directions.

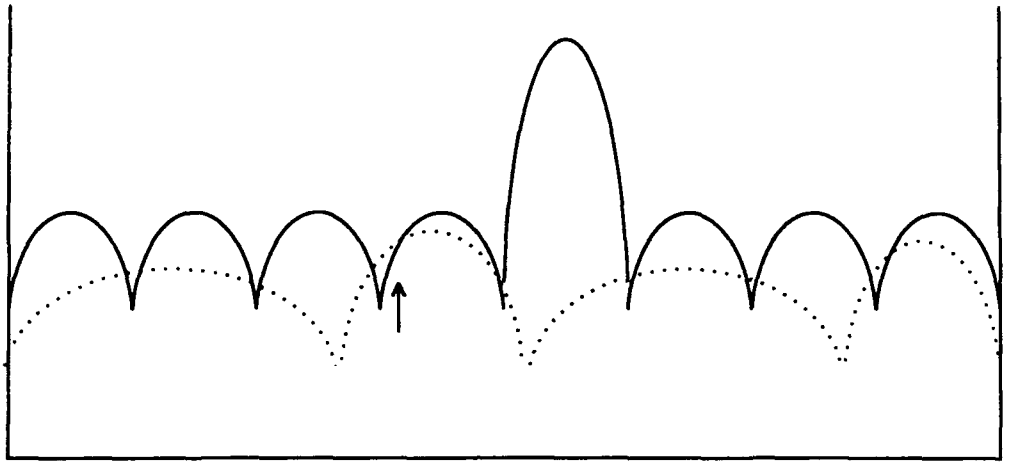

Figure 2-6 Jammer High on Sidelobes, Multiple Auxiliaries.

Figure 2-6 illustrates this case. By utilising more auxiliaries than jammers, the auxiliary pattern can be made high in the direction of the jammers and low in most other directions allowing minimal antenna response change.

This characteristic is inherent to ASLC systems.

In order to obtain the optimal weights as discussed in section 2.1 we require *a priori* knowledge of the noise environment ; given this information we would be in a position to completely remove the interfering source.

Unfortunately, in implementing ASLC on a real system, we do not have *a priori* knowledge of the noise environment and must make an estimate of the noise environment by a process of finite sampling and averaging of the incoming signals. This causes two major reductions in the overall performance of the ASLC system ; reduction in jammer suppression as the weights, having been calculated on the basis of an *estimate* of the noise environment, are no longer optimal, and a further increase in the complex weights which leads to antenna pattern degradation.

The exact magnitude of this secondary increase in complex weights is dependent on many factors but most importantly, as the number of auxiliaries in a given jammer environment increases, the sidelobes increase.

This fact tends to negate the recommendation previously ; that more auxiliaries will prevent excessive antenna pattern degradation.

Gerlach [11] refers to this excessive sidelobe degradation as *transient sidelobes* and has examined their causes, discussing the role of the covariance matrix eigenvalues in sidelobe levels and derives an expression for the average increase in sidelobe levels (ΔSL) due to finite averaging and sampling.

$$\Delta SL = \frac{G^2\sigma^2_{min}}{K-N+1}\sum_{n=1}^{N+1}\frac{1}{\lambda_n}, \quad K \geq N$$

where G is the arbitrary gain of the auxiliaries, σ^2_{min} is the minimum output noise power residue (the theoretical output of the system for an infinite number of time samples and infinite numerical

accuracy), K is the number of time samples, N is the number of auxiliaries and λ_n are the eigenvalues of the covariance matrix.

Although the above equation only makes reference to sidelobes, due to the complementary nature of sidelobes and the mainlobe, as sidelobes increase, the mainlobe gain will decrease.

As discussed earlier in section 2.3, the eigenvalues may be divided into those much greater than the noise level (*significant eigenvalues*) and those approximately equal to the noise level (*noise eigenvalues*). From the equation above, it can be seen that only the noise eigenvalues will have a significant effect on the transient sidelobe levels as the inverse of the significant eigenvalues will be much less than 1.

Gerlach defines the number of degrees of freedom (N_{DOF}) as the number of significant eigenvalues in the covariance matrix and with this definition approximates the increase sidelobe level to

$$\Delta SL \approx G^2\sigma^2_{min}\frac{N-N_{DOF}-1}{K-N+1},\ K \geq N$$

There are two main solutions to the problem of transient sidelobes ;

- Ensure the number of degrees of freedom is the same as the number of auxiliaries.
- Increase the value of the noise eigenvalues.

The first solution of estimating the number of degrees of freedom required poses many difficulties in implementation. It may be possible to generate the covariance matrix, calculate the eigenvalues, set the number of auxiliaries and then perform the ASLC. This would be a very computationally intensive solution and may cause problems in real time implementation.

The structure of the MGS sidelobe canceller shown in figure 2-2 lends itself to another form of DOF estimation. By monitoring the time averaged main channel signal power at each level of the structure it is possible to halt further decorrelation when further processing will only reduce the jammers by an insignificant amount in comparison to the increase in sidelobes.

Yuen [2] suggests that processing be stopped once the average power reaches a predetermined threshold (for example ≤ 0dB). At this point the complex weights may be calculated and applied only to those auxiliaries used in the previous decorrelation.

As DOF monitoring reduces the number of auxiliary elements, the jammer suppression will be reduced and the *inherent* sidelobe problems discussed earlier will be more prevalent.

A novel solution to the problem of excessive sidelobes due to finite averaging and sampling suggested by Gerlach is *noise injection* [11]. As shown previously, the increase in sidelobes in proportional to the sum of the inverses of the covariance matrix eigenvalues, i.e.

$$\Delta SL \propto \sum_{n=1}^{N-1}\frac{1}{\lambda_n}$$

By injecting abitrary independent noise with a noise power of σ^2 into the auxiliary channel prior to generation of the covariance matrix, the eigenvalues λ_n are increase by σ^2 which in turn modifies the expression for the change in sidelobe level to

$$\Delta SL \propto \sum_{n=1}^{N-1}\frac{1}{\lambda_n+\sigma^2}$$

For $1 << \sigma^2 << \lambda_1, \lambda_2, \ldots, \lambda_{Ndof}$ where $\lambda_1, \lambda_2, \ldots, \lambda_{Ndof}$ are the significant eigenvalues it follows that

$$\Delta SL \approx G^2\sigma^2_{min}\frac{N-N_{DOF}-1}{K-N+1}\frac{1}{\sigma^2}$$

σ^2_{min} and σ^2 should not be confused ; the first term denotes the minimum residual noise power from the ASLC system and the second term is the noise injected into the auxiliaries.

Once the complex weights are calculated they are applied to the auxiliary channels *without* the noise injection. The noise injection means that the calculated weights will not provide the suppression that would be obtained without noise injection, however, it is apparent that this technique should reduce the sidelobe levels.

A similar technique to combat excessive sidelobe increases has been suggested by Carlson [12] for use in DMI systems called *diagonal loading*. Carlson suggests a constant be added to the diagonal of the calculated covariance matrix, however, since the Gaussian noise injected into the system when utilising the noise injection is uncorrelated, noise injection also tends to add a constant to the diagonal of the covariance matrix.

It is now apparent that the tradeoff normally required between the number of auxiliaries and antenna response degradation has been eliminated. To reduce the inherent antenna response degradation that would be obtained in an optimal weights solution, as many auxiliaries as possible should be used, allowing a more directional auxiliary antenna pattern. This also improves the suppression of the jammers. To reduce excessive increases in sidelobe levels in a realistic system due to excess degrees of freedom, noise injection may be used.

The overall result will be a significant reduction of excessive sidelobe increase and mainlobe degradation at the expense of a slight reduction in jammer suppression performance.

3 SIMULATION MODELS

3.1 Antenna Elements

The antenna is modelled as a linear phased array consisting of evenly spaced isotropic elements. The number of elements in the array and the inter-element spacing are user determined. Polarisation is assumed to be linear.

The desired mainlobe to sidelobe ratio is also user determined and is achieved by Taylor weighting each antenna element before summation into the overall antenna pattern. These antenna weights have a random phase and amplitude error applied to them to simulate the errors that would be present in a real system.

The standard deviation of the amplitude error is 0.5 dB. The standard deviation of the phase error is 5°.

3.2 Noise Jammers

The jammers to be modelled in the simulation are barrage noise jammers. These jammers are forced to jam over the entire radar bandwidth and are normally circularly polarised.

The power of the jammers is specified in terms of a jammer to noise ratio per element (JNR) in the array. In order to estimate a suitable value for the JNR, the following equation may be used.

$$JNR = \frac{P_j G_j G_R \lambda^2 L_{tap}}{(4\pi R)^2 N_{elm} L_{pol} L_{aj} N_f kTB_j}$$

Jammer EIRP	$P_j G_j$	*(dBW)*
Mainlobe receiver gain	G_R	*(dBi)*
Wavelength	λ	*(m)*
Array azimuth tapering loss	L_{tap}	*(dB)*
Range to jammer	R	*(m)*
Number of elements	N_{elm}	*(-)*
Polarisation loss	L_{pol}	*(dB)*
Atmospheric attenuation	L_{aj}	*(dB)*
Noise factor	N_f	*(dB)*
Noise density	kT	*(dBW/Hz)*
Jammer bandwidth	B_j	*(Hz)*

Using the above equation, a nominal value of 35.5 dB per element has been obtained for the JNR and this value has been used extensively in the simulations.

3.3 Signal Model

This simulation uses a *narrow band* signal model. Initially the Gaussian signal from the noise jammers is generated and then used to provide a relevant signal for the antenna element.

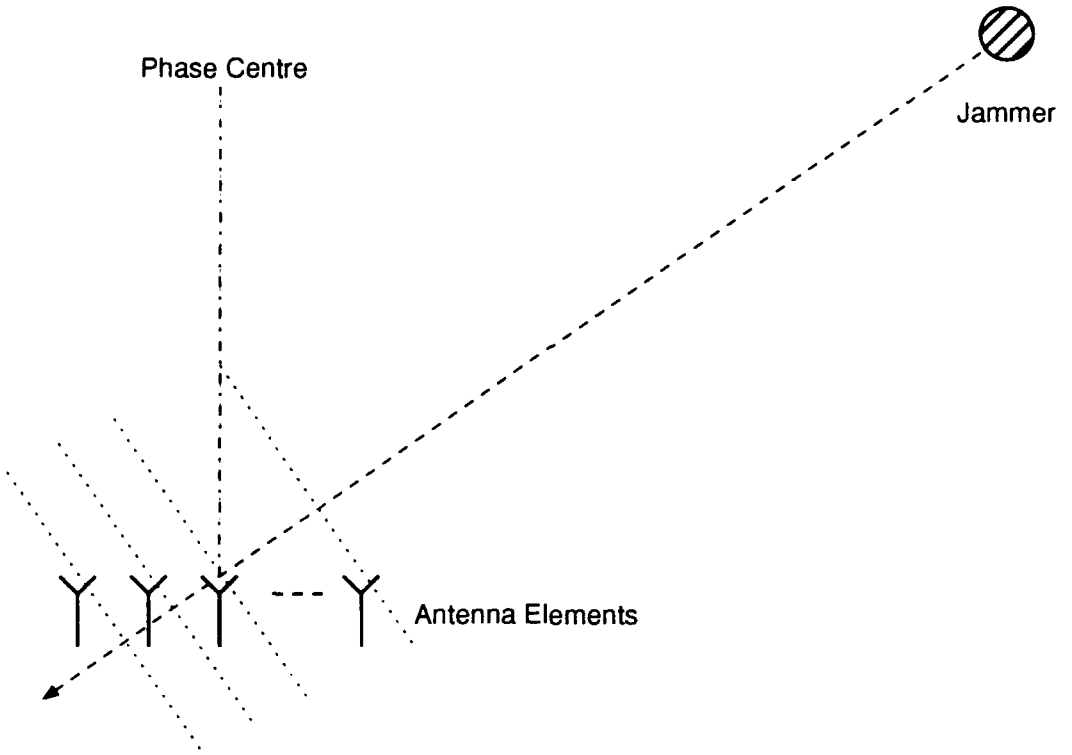

Figure 3-1 Signal Model.

Figure 3-1 shows the Gaussian signal from a typical jammer being received by the antenna elements. Having nominated a phase centre, it can be seen that at any given time, due to the geometric spacing of the antenna, each element will be receiving a different instantaneous signal voltage denoted by the dotted lines. Ordinarily a separate instantaneous signal voltage is required for each antenna element for each time slot. In order to simplify the model, only a single instantaneous signal voltage is generated per time slot and the phase of this signal is then adjusted to reflect the geometric path difference between elements. This simplification assumes the jammer is at a single frequency hence the descriptor *narrow band.*

3.4 Receiver Hardware

The receiver hardware model has been greatly simplified in order to speed progress. Real radar systems comprise low noise amplifiers, band-pass filters and other components that modify the signal between reception by the antenna and processing of the data. The only consideration towards a real radar system is the inclusion of the random phase and amplitude errors applied to the Taylor weights as discussed in section 3.1.

4 RESULTS

4.1 Introduction

The results have been obtained from two software packages ; ASLC_DMI written previously by Ericsson Radar Electronics in Sweden, and ASLC_GS written as part of this project. For all cases examined, the following basic radar parameters have been used.

- Number of Elements 192
- Element spacing 0.04 m
- Centre frequency 3 GHz
- Taylor Weight SLL 50 dB
- Samples in full data set 512
- Samples in reduced data set 64
- Noise injection level (when used) 10 dBN
- Weight scaling constraint 1.0
- Weight zeroise constraint 5.0

The last two parameters constrain the weights in order to prevent excessive degradation of the antenna pattern. If any of the complex weights has a magnitude exceeding *weight scaling constraint* then all weights are scaled so that the largest weight has a magnitude equal to *weight scaling constraint*. If any of the complex weights has a magnitude exceeding *weight zeroise constraint*, all the weights are set to 0 and thus ASLC is not applied.

Information unique to each case includes.

- Number of auxiliary elements.
- Positions of the auxiliary elements.
- Number of jammers.
- Directions of arrival for each jammer.
- Jammer to noise ratio per element for each jammer.

All cases have been averaged over 100 trials unless noted in order to reduce the chance of statistical anomalies affecting the conclusions.

4.2 Performance Measures

In order to assess and compare the performance of various ASLC algorithms, several performance measures are calculated during the simulation.

- *Initial gain* : This is the antenna gain in the direction of the jammer. When compared with the final gain, the null depth may be calculated.
- *Initial average sidelobe level* : Once the antenna elements have been Taylor weighted, the average sidelobe level can be calculated. The fraction of the antenna pattern containing the main lobe is ignored. For any given simulation, the initial average sidelobe level is constant and is calculated at the beginning of the simulation. This calculation allows the sidelobe degradation to be examined.

- *Initial received power* : This represents the power received in the main channel before any ASLC processing over a complete data set (512 samples). The figure given is referenced to the noise level, hence the units dBN. In all simulations, the noise component is normalised to unity (0 dBN).
- *Final average sidelobe level* : The complex weights calculated by the ASLC algorithm are incorporated into the sidelobe calculations in order to obtain an average sidelobe level after ASLC. This value is averaged over all the trials of a jammer configuration.
- *Increase in sidelobe levels* : This value is the initial average sidelobe level subtracted from the final average sidelobe level.
- *Final mainlobe level* : This figure gives the gain of the mainlobe after ASLC ; as no steering has been implemented this corresponds to the gain at 0^{o} on the antenna diagram.
- *Reduction in mainlobe level* : This is the final mainlobe level subtracted from the intial mainlobe level (for all cases, the initial mainlobe level is 21.21 dBi).
- *Final signal level* : Having subtracted the weighed auxiliary signals from the main channel, the power remaining in the main channel is the final signal level. This value is averaged over all the trials of a jammer configuration and is given in terms of the noise level (dBN).
- *Final signal level - noise* : This value is the final signal level with the noise component removed. It represents the amount of jammer interference remaining in the main channel after ASLC and is also given in terms of the noise level (dBN).
- *Auxiliary gain* : The complex weights calculated by the ASLC algorithm, in conjunction with the auxiliary elements, form the auxiliary antenna pattern. The auxiliary gain is the gain of the auxiliary antenna pattern in the direction of the jammers. The auxiliary gain should be as close to the initial gain as possible to ensure maximum null depth.
- *Final gain* : The antenna gain in the direction of the jammer after ASLC.
- *Eigenvalues* : The eigenvalues of the covariance matrix $\underline{M}$ have been calculated in order to illustrate the principle of significant and noise eigenvalues.
- *Condition number* : By dividing the maximum and minimum eigenvalues of the covariance matrix M, the eigenvalue spread or condition number of $\underline{M}$ can be obtained. This gives an indication of the ill-conditioning of the system.

4.3 DMI vs MGS

4.3.1 Case 1

Both DMI and MGS attempt to solve the Weiner-Hopf equation in order to obtain the complex weights. As such, in most cases one would expect identical results for both methods ; only for those scenarios discussed previously would differences be observed.

This first point is shown in appendix A. The two cases are for identical antennas with identical jammer scenarios, however, the first suppresses the jammers using the DMI algorithm and the second using MGS. The antenna and jammer scenario was chosen in order to provide a well conditioned covariance matrix to avoid the problems of DMI.

Both algorithms are provided with identical jammer signals in order to provide an exact comparison of algorithm performance. As a result, both algorithms produced identical results. The eigenvalue spread of 4.59 is apparently too low to cause any matrix ill-conditioning problems.

4.3.2 Case 2

Section 2.3 discusses the problem of matrix ill-conditioning with the DMI algorithm. The theory predicted that errors in the weights, leading to reduced jammer suppression would result from covariance matrix ill-conditioning. This ill-conditioning occurs when there is a large difference between the significant eigenvalues and the noise eigenvalues in the covariance matrix which results in a large eigenvalue spread.

The results in appendix B attempt to highlight this problem. Both simulations involve a 10 auxiliary adaptive array in the presence of two jammers. The eigenvalues of the system clearly show the division between the two significant eigenvalues and the remaining eight noise eigenvalues. This results in an eigenvalue spread of 2.8×10^6.

The important values are the average final signal powers for both DMI and MGS ; the final signal level in the DMI system is 3.91 dBN while MGS has reduced the signal level to below the noise level. Comparing the null depth for both cases, the nulls obtained using MGS are approximately 16 dB lower then the DMI nulls.

4.3.3 Case 3

The ill-conditioning problems of DMI are further illustrated by the results shown in appendix C. In this case, an identical jammer scenario as that in the previous example is suppressed by 20 auxiliaries.

As the total of the eigenvalues is equal to the sum of the power received by the auxiliaries, it is expected that the largest eigenvalue with 20 auxiliaries will be larger than the largest eigenvalue in a 10 auxiliary system. This is indeed the case (2308643 compared with 1841576) and as the condition number is correspondingly larger (4.6×10^6compared with 2.8×10^6), the suppression performance of a 20 auxiliary DMI system is significantly worse than for a 10 auxiliary system.

The final signal level is now 13.87 dBN ; a increase of almost 10 dB over the 10 auxiliary system.

MGS on the other hand has improved its jammer suppression performance slightly over the 10 auxiliary system. As MGS does not suffer from matrix ill-conditioning, adding extra auxiliaries only increases the ability of the system to suppress jammer interference.

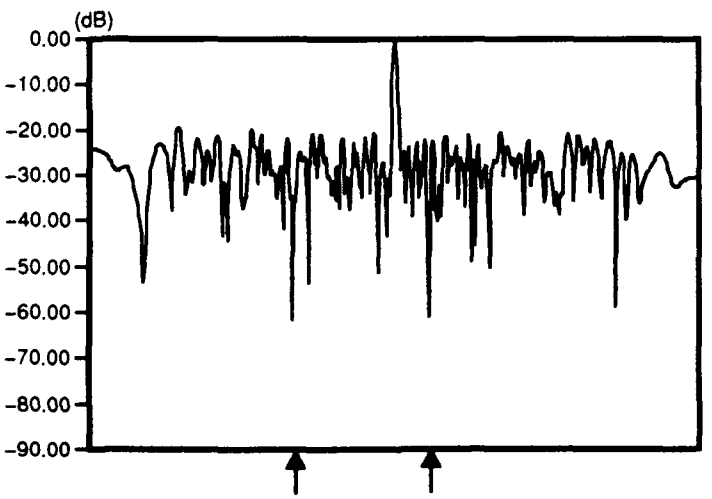

Figure 4-1 20 Auxiliaries and 2 Jammers - DMI Algorithm

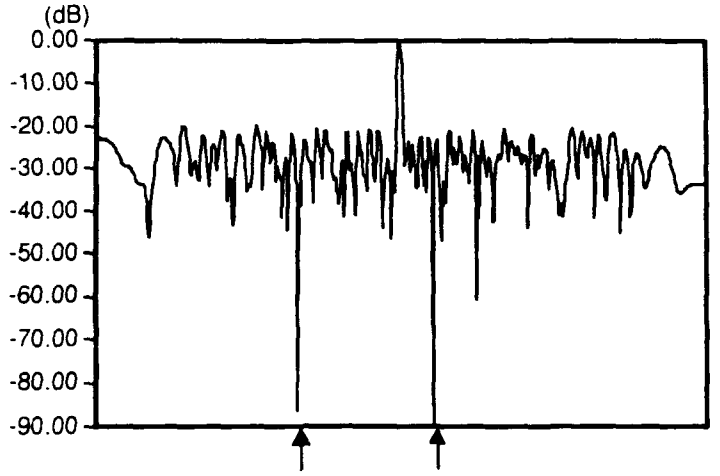

Figure 4-2 20 Auxiliaries and 2 jammers - MGS Algorithm

Figures 4-1 and 4-2 show the advantages of MGS clearly. Figure 4-1 shows the antenna pattern for case 3 after ASLC using the DMI algorithm. The antenna diagram is from - 90° to + 90° and has been normalised so that the main lobe gain is 0 dB. The positions of the jammers are indicated by the arrows. Comparing this to figure 4-2, which is also the antenna diagram for case 3 but using the MGS algorithm, the arrows clearly show the improvement in null depth achieved with MGS.

4.3.4 Case 4

The average effect of increasing the eigenvalues on the DMI algorithm is shown clearly in figure 4-3 with a plot of received power after ASLC against eigenvalue spread.

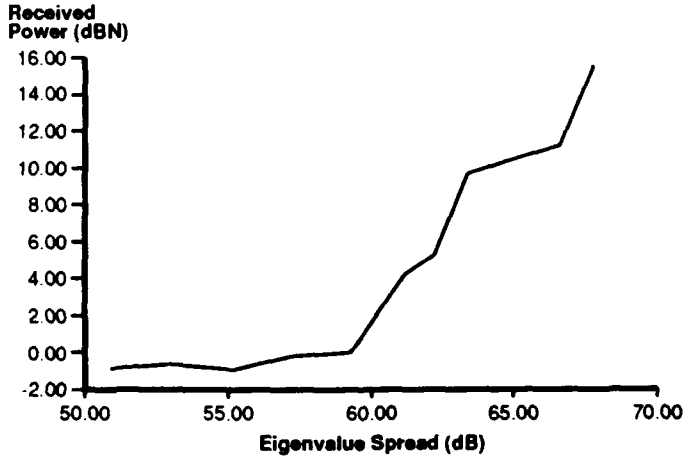

Figure 4-3 Eigenvalue Spread vs Received Power.

The scenario under examination is identical to the previous system with 20 auxiliaries suppressing 2 jammers. Jammer powers of between 40 dBN to 51 dBN have been used in order to obtain a wide range of eigenvalue spread. The results used to create this graph are contained in appendix D.

The graph shows clearly the concept of a *critical* value of eigenvalue spread discussed in section 2.3. In this case, that critical value corresponds to an eigenvalue spread of approximately 1×10^6.

Reviewing the values in appendix D, it must also be noted that visible matrix ill-conditioning effects occur with only a 1 dB increase in the jammer powers.

4.4 Antenna Response Degradation

The subject of sidelobes was discussed in section 2.5. It was proposed that excessive sidelobe increases and mainlobe degradation would result from having a high average auxiliary sidelobe level which occurs when trying to suppress jammers high in the unadapted sidelobes. The following cases utilising MGS illustrate this point.

4.4.1 Case 5

This proposal is supported by the results in appendix E. Identical antenna systems are attempting to suppress two different jammer scenarios ; one with the jammers high on the adapted sidelobes and one with the jammers low on the unadapted sidelobes.

As expected there is a significant difference in the increase in sidelobe levels ; 13.51 dB for the jammers high on the sidelobes against 5.38 dB for the jammers low on the sidelobes. In association with these increases are the decreases in the mainlobe ; 4.66 dB for the jammers high on the sidelobes against 0.34 dB for the jammers low in the sidelobes. A comparison of the final signal powers reveals very little difference in the suppression for each case (0.22 dBN compared with 0.16 dBN) despite the difference in inital signal power.

4.4.2 Case 6

By increasing the number of auxiliaries, it is possible to reduce the sidelobe increase and mainlobe decrease due to the increased selectivity of the auxiliary pattern. Unfortunately, having more auxiliaries that jammers (i.e. having excess degrees of freedom) exaggerates antenna pattern degradation caused by finite sampling and averaging.

Appendix F contains the results of a simulation with a 20 auxiliary ASLC system attempting to suppress the two previous jammer scenarios.

As the main contributing factor to the high sidelobes is the excess degrees of freedom shared by both cases, the resulting sidelobe levels are very similar ; 10.76 dBi for the jammers high in the sidelobes and 10.52 dBi for the jammers low in the sidelobes. As there are many more auxiliaries than jammers, the position of the jammers on the sidelobes becomes less important.

Similarly, both cases show sizeable reductions in mainlobe gain ; 3.15 dB for the jammers high on the sidelobes and 1.41 dB for the jammers low in the sidelobes. Again the suppression performance of both scenarios is virtually identical and as expected the 20 auxiliary case suppression has improved slightly on the 4 auxiliary case.

The effect of increasing the number of degrees of freedom in an ASLC system is shown in figure 4-4.

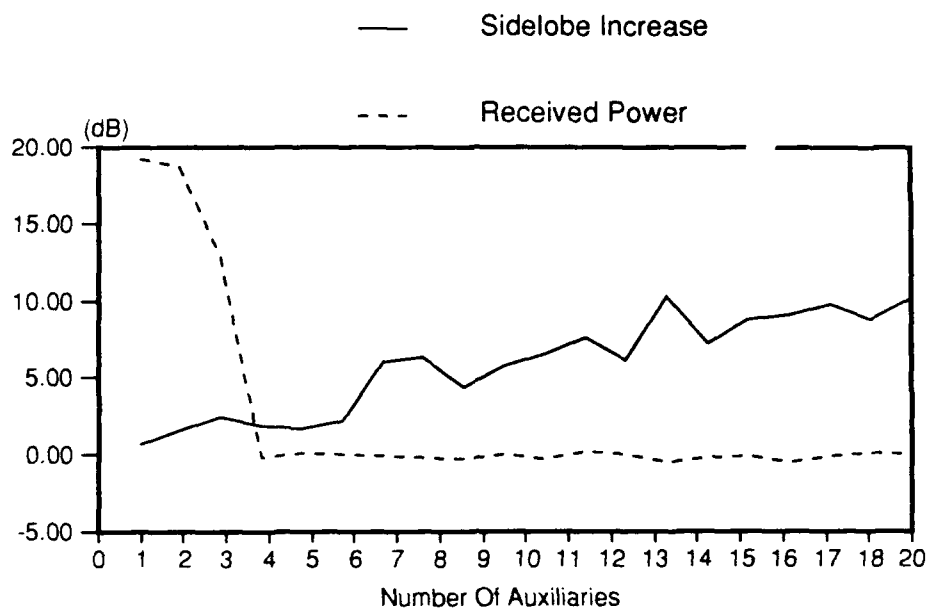

Figure 4-4 Sidelobes and Received Power vs Auxiliaries - No Noise Injection

The graph shows the results of simulating the suppression of a 4 jammer environment with between 1 and 20 auxiliaries ; the results are contained in appendix G.

The suppression performance, represented by the dotted received power line, improves dramatically as the number of auxiliaries equals the number of jammers and there are no excess degrees of freedom. As the number of auxiliaries increases from 4 to 20, there is no significant improvement in jammer suppression as the jammers have already been suppressed to below the noise level.

The sidelobes, however, increase steadily as the number of excess degrees of freedom increases with the number of auxiliaries.

To reduce the excessive sidelobe increases caused by excess degrees of freedom, the technique of noise injection may be used. By injecting Gaussian noise into the auxiliary channels when calculating the weights, a constant equal to the noise power density of the injected noise is added to the noise eigenvectors which reduces the sidelobe increase caused by finite sampling and averaging.

The results shown in figure 4-4 have been re-simulated with 10 dBN of Gaussian noise injected into the auxiliary channels prior to calculation of the weights. The results of this simulation are shown in figure 4-5 and tabulated in appendix H.

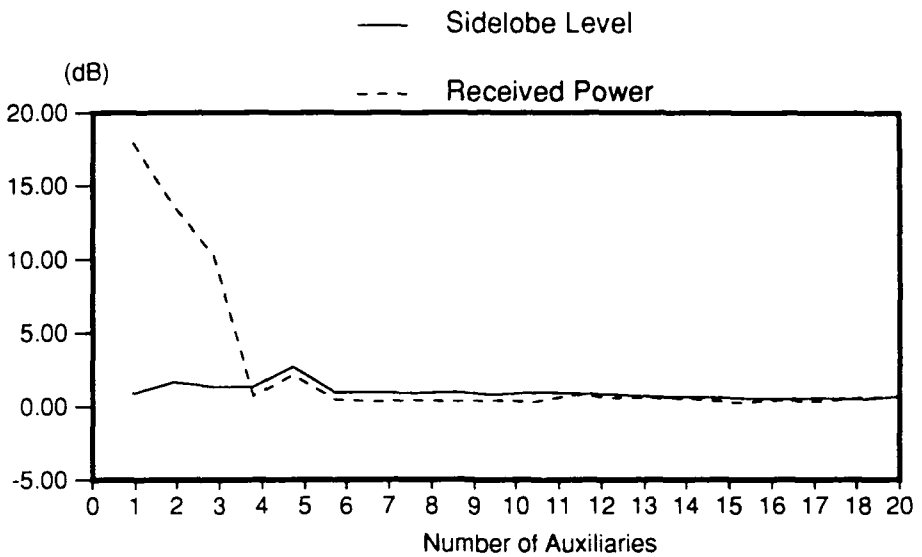

Figure 4-5 Sidelobes and Received Power vs Auxiliaries - 10 dBN Noise Injection

The rapid reduction in the received power is consistent with the previous example which did not utilise noise injection. The major difference is in the sidelobe levels, with noise injection clearly reducing the link between the number of degrees of freedom and the excessive sidelobe increase.

Closer comparison of the data in appendices G and H reveals that the jammer suppression obtained by the noise injected simulation is not quite as good as that obtained without noise injection. Ignoring the first three results as there are insufficient auxiliaries for the number of jammers, the noise injected received powers averaged 0.66 dB above the received power without noise injection and the noise injected sidelobe levels averaged 5.78 dB below the sidelobe levels without noise injection.

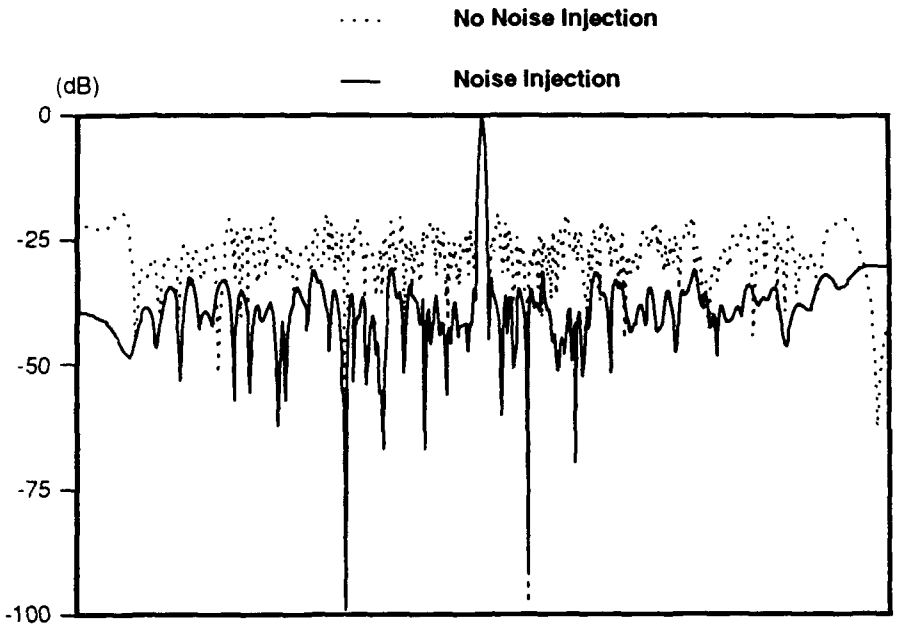

Figure 4-6 Noise Injection and No Noise Injection.

4.4.3 Case 7

Figure 4-6 shows the antenna diagrams for case 2 with both the noise injected and non-noise injected algorithms displayed. The antenna diagrams have been normalised so that the mainlobe gain is unity (0 dB). The difference in average sidelobe levels is quite apparent (26.16 dB below the mainlobe without noise injection, 37.55 dB below the mainlobe with noise injection) and noise injection also reduces the mainlobe degradation (-1.21 dB without noise injection, - 0.02 dB with noise injection), however, there is a slight reduction in the null depths. A full summary of the results for this example appears in appendix I.

From the results given in section 4.4, the effectiveness of noise injection in reducing excessive sidelobe increases and mainlobe degradation due to excess degrees of freedom can be seen. It may therefore be concluded that a multiple auxiliary ASLC system with noise injection will provide excellent suppression characteristics without significantly degrading the antenna pattern response.

5 CONCLUSIONS

This report is the final component of a study of adaptive sidelobe cancelling techniques carried out at DSTO in 1991. It was hoped that the study would provide an opportunity to learn about ASLC techniques as well as some of the practical considerations that need to be taken in account when designing an ASLC system for use in radar. Specifically, the study sought to find a suitable algorithm for implementation on a large phased array and to evaluate its performance.

Previous studies into ASLC have been carried out by Ericsson Radar Electronics in Sweden and simulation software for the DMI algorithm was available for the purposes of comparison. After an extensive literature search [14], the modified Gram-Schmidt algorithm was chosen for this study.

The literature survey also revealed some of the recent innovations in ASLC. The maintenance of the original antenna pattern using noise injection was incorporated into the study as well as the understanding of many ASLC properties in terms of eigenvalues and eigenvectors.

A major part of the project involved writing software to simulate a phased array utilising the MGS algorithm for ASLC. The software generated suitable jammer signals which were received by the array. The received signals were then passed to the ASLC algorithm which performed the cancellation. Degradation of the antenna pattern was restricted by including noise injection in the algorithm. Extensive evaluation of the algorithm performance was included in the software and these results subsequently output to files.

Once the software was completed, a variety of jammer and auxiliary configurations were simulated in order to compare MGS with DMI. The theory behind both algorithms points to their performance being identical for the majority of jammer and auxiliary configurations and results provided by the simulation software agreed with the theoretical predictions. Only when the array has excess degrees of freedom in the presence of strong jamming interference, are the advantages provided by MGS visible.

The benefits of noise injection were also examined via simulation. The ability of noise injection to reduce excessive sidelobe increases and mainlobe degradation associated with excess degrees of freedom without significantly degrading jammer suppression was demonstrated, however, this raises questions about using this procedure.

There are many trade-offs in radar system design and noise injection introduces another ; antenna response degradation versus jamming suppression.

The use of noise injection in a radar system, illustrates this point. Detection of targets is a function of the signal to noise ratio and both clutter *and* jamming increase the noise floor in the receive path.

In a high clutter environment, it may be that the noise component from sidelobe clutter exceeds the noise from the ASLC suppressed jammers and noise injection will reduce the *overall* noise entering the system.

On the other hand, in a low clutter environment or with a high PRF, the overall signal to noise ratio may be best served by turning off noise injection and obtaining better jammer suppression.

This introduces the concept of adaptive ASLC in which the parameters of the ASLC algorithm are dynamically adapted to the current system environment and tailored to the specific application. Such control would increase the performance of ASLC without degrading the overall performance of the system utilising ASLC.

REFERENCES

1. Applebaum, S. P. Adaptive Arrays. IEEE Transactions on Antenna and Propagation. Sept 1976. pp 585 - 598.
2. Yuen, S.M. Algorithmic, Archtectural and Beam Pattern Issues of Sidelobe Cancellation. IEEE Transactions on Aerospace and Electronic Systems, July 1984. pp 459 - 471.
3. Widrow et Al. Adaptive Antenna Systems. Proceedings of the IEEE, Dec 1967. pp 2143 - 2159.
4. Reed et Al. Rapid Convergence Rates in Adaptive Arrays. IEEE Transactions on Aerospace and Electronics Systems. Nov 1974. pp 853 - 863.
5. Morgan, D.E. Partially Adaptive Array Techniques. IEEE Transactions on Antennas and Propagation, Nov 1978. pp 823 - 833.
6. Jordan, T.L. Experiments on Error Growth Associated with some Linear Least Squares Procedures. Mathematical Computations, Vol 20 1966. pp 325 - 338.
7. Wilkinson, J.H. Rounding Errors in Algebraic Processes. Prentice Hall, New Jersey, 1963. pp 79-93.
8. Faddeev, D.K. and Faddeeva, V.N. Computational Methods of Linear Algebra. W.H. Freeman and Co. London, 1963. p 126.
9. Monzingo and Miller. Introduction to Adaptive Arrays. John Wiley and Sons, New York. pp 312 - 313.
10. Compton, R. T. Adaptive Antennas. Prentice Hall Inc, London, 1988. pp 258 - 271.
11. Gerlach, K. Adaptive Array Transient Sidelobe Levels and Remedies. IEEE Transactions on Aerospace and Electronic Systems, May 1990. pp 560 - 568.
12. Carlson, B. D. Covariance Matrix Estimation Errors and Diagonal Loading in Adaptive Arrays. IEEE Transactions on Aerospace and Electronic Systems, July 1988. pp 397 - 401.
13. Ward, J. and Compton, R.T. Jnr. Sidelobe Level Performance of Adaptive Sidelobe Canceller Arrays with Element Reuse. IEEE Transactions on Antenna and Propagation, October 1990. pp 1684 - 1693.
14. Stone, M. Report on Literature Survey on ASLC Algorithms. DSTO Technical Memo, 1991.

Appendix A : 4 Auxiliaries, 4 Jammers

Case Details

- Number of auxilaries 4
- Positions of auxiliaries 5,35,158,188
- Number of jammers 4
- Eigenvalues 5313, 10617, 17918, 24411
- Condition Number 4.59

Jammer	Direction of Arrival	Jammer to Noise Ratio (dBN)	Initial Gain (dBi)
1	- 45°	35.5	- 21.61
2	- 30°	35.5	- 19.37
3	+ 20°	35.5	- 19.61
4	+ 40°	35.5	- 20.93

- Initial Average Sidelobe Level - 17.15 dBi
- Initial Received Power + 21.26 dBN

DMI

- Final Average Sidelobe Level - 16.34 dBi
- Increase in Sidelobe Level + 0.81 dB
- Final Signal Level + 0.23 dBN
- Final Signal Level - Noise - 12.55 dB

Jammer	Auxiliary Gain (dBi)	Final Gain (dBi)
1	- 21.60	- 53.54
2	- 19.38	- 53.70
3	- 19.63	- 52.84
4	- 20.93	- 53.35

MGS

- Final Average Sidelobe Level - 16.34 dBi
- Increase in Sidelobe Level + 0.81 dB
- Final Signal Level + 0.23 dBN
- Final Signal Level - Noise - 12.55 dB

Jammer	Auxiliary Gain (dBi)	Final Gain (dBi)
1	- 21.60	- 53.54
2	- 19.38	- 53.70
3	- 19.63	- 52.84
4	- 20.93	- 53.35

Appendix B : 10 Auxiliaries, 2 Jammers

Case Details

- Number of auxilaries 10
- Positions of auxiliaries 5, 25, 35, 50, 65, 80, 95,110,125,140
- Number of jammers 2
- Eigenvalues 1841576, 266711, 1.357, 0.656, 0.749, 1.163, 0.847, 0.914, 1.052, 1.014
- Condition Number 2.8×10^6

Jammer	Direction of Arrival	Jammer to Noise Ratio (dBN)	Initial Gain (dBi)
1	- 30°	50.0	- 19.37
2	+ 10°	50.0	- 17.97

- Initial Average Sidelobe Level - 17.15 dBi
- Initial Received Power + 34.37 dBN

DMI

- Final Average Sidelobe Level - 8.91 dBi
- Increase in Sidelobe Level + 8.24 dB
- Final Signal Level + 3.91 dBN
- Final Signal Level - Noise - 1.64 dB

Jammer	Auxiliary Gain (dBi)	Final Gain (dBi)
1	- 19.43	- 51.03
2	- 18.04	- 51.44

MGS

- Final Average Sidelobe Level - 8.99 dBi
- Increase in Sidelobe Level + 8.16 dB
- Final Signal Level - 0.09 dBN
- Final Signal Level - Noise ≈ 0

Jammer	Auxiliary Gain (dBi)	Final Gain (dBi)
1	- 19.37	- 67.97
2	- 17.97	- 68.04

Appendix C : 20 Auxiliaries, 2 Jammers

Case Details

- Number of auxilaries: 20
- Positions of auxiliaries: 5, 14, 24, 33, 43, 52, 62, 71, 81, 90, 100, 119, 128, 138, 147, 157, 166, 176, 188
- Number of jammers: 2
- Eigenvalues: 2308643, 1812892, 1.513, 0.500, 1.414, 0.637, 0.661, 0.696, 0.744, 1.330, 0.850, 0.910, 0.915, 0.950, 1.044, 1.077, 1.237, 1.198, 1.174, 1.160
- Condition Number: 4.6×10^6

Jammer	Direction of Arrival	Jammer to Noise Ratio (dBN)	Initial Gain (dBi)
1	- 30°	50.0	- 19.37
2	+ 10°	50.0	- 17.97

- Initial Average Sidelobe Level - 17.15 dBi
- Initial Received Power + 34.37 dBN

DMI

- Final Average Sidelobe Level - 6.02 dBi
- Increase in Sidelobe Level + 11.13 dB
- Final Signal Level + 13.87 dBN
- Final Signal Level - Noise + 13.69 dB

Jammer	Auxiliary Gain (dBi)	Final Gain (dBi)
1	- 19.73	- 39.45
2	- 18.39	- 39.09

MGS

- Final Average Sidelobe Level - 6.16 dBi
- Increase in Sidelobe Level + 10.99 dB
- Final Signal Level - 0.83 dBN
- Final Signal Level - Noise ≈ 0

Jammer	Auxiliary Gain (dBi)	Final Gain (dBi)
1	- 19.37	- 69.06
2	- 17.97	- 69.00

Appendix D : Eigenvalues vs Received Power

Case Details

- Number of auxilaries 20
- Positions of auxiliaries 5, 14, 24, 33, 43, 52, 62, 71, 81, 90, 100, 119, 128, 138, 147, 157, 166, 176, 188
- Number of jammers 2
- Position of jammers -30°, 10°
- Number of trials 10

Jammer Strength (dBN)	Eigenvalue Spread	Eigenvalue Spread (dB)	Received Power (dBN)
36	122429	50.9	- 0.86
38	200430	53.0	- 0.63
40	327454	55.2	- 0.91
42	527661	57.2	- 0.16
44	842978	59.3	+ 0.04
46	1306914	61.2	+ 4.25
47	1676293	62.2	+ 5.29
48	2187908	63.4	+ 9.66
49	3115488	64.9	+ 10.44
50	4619493	66.6	+ 11.24
51	5968466	67.8	+ 15.56

Appendix E : 4 Auxiliaries, 4 Jammers

Case Details

- Number of auxilaries 4
- Positions of auxiliaries 5, 35, 158, 188
- Number of jammers 4
- Jammer to noise ratios 35.5
- Initial Average Sidelobe Level - 17.15 dBi
- Initial Mainlobe Level 21.21 dBi

Jammers High on Sidelobes

Jammer	Direction of Arrival	Initial Gain (dBi)	Final Gain (dBi)
1	- 36.00°	- 11.98	-52.75
2	- 19.80°	- 11.67	-52.54
3	+ 10.80°	- 12.60	-53.91
4	+ 46.80°	- 10.64	-53.38

- Initial Received Power + 29.86 dBN
- Final Average Sidelobe Level - 3.64 dBi
- Increase in Sidelobe Level + 13.51 dB
- Final Mainlobe Level + 16.55 dBi
- Reduction in Mainlobe Level - 4.66 dB
- Final Signal Level + 0.22 dBN
- Final Signal Level - Noise - 12.76 dB

Jammers Low on Sidelobes

Jammer	Direction of Arrival	Initial Gain (dBi)	Final Gain (dBi)
1	- 33.84°	- 27.42	-53.07
2	- 21.24°	- 38.17	-53.20
3	+ 15.48°	- 29.74	-54.08
4	+ 43.20°	- 37.35	-53.05

- Initial Received Power + 10.88 dBN
- Final Average Sidelobe Level - 11.78 dBi
- Increase in Sidelobe Level + 5.38 dB
- Final Mainlobe Level + 20.87 dBi
- Reduction in Mainlobe Level - 0.34 dB
- Final Signal Level + 0.16 dBN
- Final Signal Level - Noise - 14.27 dB

Appendix F : 20 Auxiliaries, 4 Jammers

Case Details

- Number of auxilaries 20
- Positions of auxiliaries 5, 14, 24, 33, 43, 52, 62, 71, 81, 90, 100, 119, 128, 138, 147, 157, 166, 176, 188
- Number of jammers 4
- Jammer to noise ratios 35.5
- Initial Average Sidelobe Level - 17.15 dBi
- Initial Mainlobe Level + 21.21 dBi

Jammers High on Sidelobes

Jammer	Direction of Arrival	Initial Gain (dBi)	Final Gain (dBi)
1	- 36.00°	- 11.98	-54.04
2	- 19.80°	- 11.67	-53.20
3	+ 10.80°	- 12.60	-52.56
4	+ 46.80°	- 10.64	-53.21

- Initial Received Power + 29.83 dBN
- Final Average Sidelobe Level - 6.39 dBi
- Increase in Sidelobe Level + 10.76 dB
- Final Mainlobe Level + 18.06 dBi
- Reduction in Mainlobe Level - 3.15 dB
- Final Signal Level - 0.03 dBN
- Final Signal Level - Noise ≈ 0

Jammers Low on Sidelobes

Jammer	Direction of Arrival	Initial Gain (dBi)	Final Gain (dBi)
1	- 33.84°	- 27.42	-54.28
2	- 21.24°	- 38.17	-53.25
3	+ 15.48°	- 29.74	-52.85
4	+ 43.20°	- 37.35	-53.14

- Initial Received Power + 10.89 dBN
- Final Average Sidelobe Level - 6.63 dBi
- Increase in Sidelobe Level + 10.52 dB
- Final Mainlobe Level + 19.80 dBi
- Reduction in Mainlobe Level - 1.41 dB
- Final Signal Level - 0.04 dBN
- Final Signal Level - Noise ≈ 0

Appendix G : Sidelobes - No Noise Injection

Case Details

- Numbers of Auxiliaries: 1 - 20
- Auxiliary Positions: 9, 180, 18, 171, 27, 162, 36, 153, 45, 144, 54, 135, 63, 126, 72, 117, 81, 108, 90, 99 (Order in which auxiliaries are implemented)
- Number of Jammers: 4
- Positions of jammers: -45°, -30°, 20°, 40°
- Jammer Powers: 35.5 dBN
- Number of Trials: 5

Number of Auxiliaries	Increase in Sidelobes (dB)	Received Power (dBN)
1	0.66	+19.17
2	1.62	+18.70
3	2.46	+12.80
4	1.93	-0.15
5	1.66	+0.09
6	2.19	+0.02
7	6.05	-0.08
8	6.34	-0.17
9	4.36	-0.30
10	5.69	-0.03
11	6.49	-0.29
12	7.60	+0.24
13	6.11	-0.03
14	10.21	-0.44
15	7.20	-0.19
16	8.76	-0.08
17	9.03	-0.47
18	9.73	-0.09
19	8.76	+0.11
20	10.15	+0.04

Appendix H : Sidelobes - 10 dBN Noise Injection

Case Details

- Numbers of Auxiliaries: 1 - 20
- Auxiliary Positions: 9, 180, 18, 171, 27, 162, 36, 153, 45, 144, 54, 135, 63, 126, 72, 117, 81, 108, 90, 99 (Order in which auxiliaries are implemented)
- Number of Jammers: 4
- Positions of jammers: -45°, -30°, 20°, 40°
- Jammer Powers: 35.5 dBN
- Number of Trials: 5

Number of Auxiliaries	Increase in Sidelobes (dB)	Received Power (dBN)
1	0.86	17.96
2	1.67	13.59
3	1.38	10.25
4	1.34	0.69
5	2.66	2.12
6	0.95	0.47
7	0.96	0.35
8	0.85	0.40
9	0.94	0.30
10	0.80	0.39
11	0.97	0.31
12	0.85	0.79
13	0.82	0.59
14	0.66	0.54
15	0.61	0.44
16	0.53	0.25
17	0.49	0.36
18	0.54	0.32
19	0.47	0.55
20	0.65	0.64

Appendix I : 20 Auxiliaries, 2 Jammers

Case Details

- Number of auxilaries: 20
- Positions of auxiliaries: 5, 14, 24, 33, 43, 52, 62, 71, 81, 90, 100, 119, 128, 138, 147, 157, 166, 176, 188
- Number of jammers: 2
- Eigenvalues: 2308643, 1812892, 1.513, 0.500, 1.414, 0.637, 0.661, 0.696, 0.744, 1.330, 0.850, 0.910, 0.915, 0.950, 1.044, 1.077, 1.237, 1.198, 1.174, 1.160
- Condition Number: 4.6×10^6

Jammer	Direction of Arrival	Jammer to Noise Ratio (dBN)	Initial Gain (dBi)
1	- 30°	50.0	- 19.37
2	+ 10°	50.0	- 17.97

- Initial Average Sidelobe Level - 17.15 dBi
- Initial Mainlobe Level + 21.21 dBi
- Initial Received Power + 34.37 dBN

No Noise Injection

- Final Average Sidelobe Level - 6.16 dBi
- Increase in Sidelobe Level + 10.99 dB
- Final Mainlobe Level + 20.00 dBi
- Reduction in Mainlobe Level - 1.21 dB
- Final Signal Level - 0.83 dBN
- Final Signal Level - Noise ≈ 0

Jammer	Auxiliary Gain (dBi)	Final Gain (dBi)
1	- 19.37	- 69.06
2	- 17.97	- 69.00

Noise Injection

- Final Average Sidelobe Level - 16.36 dBi
- Increase in Sidelobe Level + 0.79 dB
- Final Mainlobe Level + 21.19 dBi
- Reduction in Mainlobe Level - 0.02 dB
- Final Signal Level - 0.18 dBN
- Final Signal Level - Noise - 13.82 dBN

Jammer	Auxiliary Gain (dBi)	Final Gain (dBi)
1	- 19.36	- 65.26
2	- 17.97	- 65.65

Distribution List

	No. of copies
Defence Science and Technology Organisation	
Chief Defence Scientist and members of the	1
DSTO Central Office Executive (shared copy)	
Main Library (DSTOS)	2
Surveillance Research Laboratory	
Director Surveillance Research Laboratory (DSRL)	1
Chief Microwave Radar Division (CMRD)	1
Head Radar Concepts and Capabilities (HRCC)	1
Dr L. Powis (RCC)	1
Mr P. Sarunic (RCC)	1
Mr D. Lambert (RCC)	1
AGPS	1
CONDS(W)	Document Control Data Sheet
CONDS(L)	Document Control Data Sheet
Navy Scientific Adviser (NSA)	1
Scientific Adviser - Army (SA-A) 1	
Air Force Scientific Adviser (AFSA)	1
Scientific Adviser - Defence Central (SA-DC)	1
Defence Central Library - Technical Reports Centre	1
Manager Document Exchange Centre (MDEC) (for retention)	1
Defence Research Information Centre United Kingdom	2
National Technical Information Sevice United States	2
Director Scientific Information Services Canada	1
Ministry of Defence New Zealand	1
National Library of Australia	1
British Library, Document Supply Centre	1
SA - DIO	1
Library DSD	1
Ericsson Defence Systems	
Mr I. Trayling, EDM/C. (for retention)	1
Ericsson Defence Systems.	
P.O. Box 264, Preston 3072	
Mr J. Daly (DICD) 1	
Mr A. Norris (DIDO)	1
Mr M. Heed (Ericsson Radar Electronics)	1
Mr J. Nilsson (Ericsson Radar Electronics)	1
Mr H. Hindsefelt (Förvarets Materielverk, Radarbyrån)	1
Mr B. Andersson (Communicator Sensonik AB)	1
Ms Å. Jakobsson, EDM/DC.	1
Mr M. Stone EDM/D.	1

DOCUMENT CONTROL DATA SHEET

Security classification of this page : UNCLASSIFIED

1 DOCUMENT NUMBERS

AR Number : AR-006-969

Series Number : SRL-0096-TR

Other Numbers :

2 SECURITY CLASSIFICATION

a. Complete Document : Unclassified

b. Title in Isolation : Unclassified

c. Summary in Isolation : Unclassified

3 DOWNGRADING / DELIMITING INSTRUCTIONS

N/A

4 TITLE

REAL TIME DATA REFORMATTING USING THE TMS320C25 DEVELOPMENT SYSTEM

5 PERSONAL AUTHOR (S)

M. STONE

6 DOCUMENT DATE

March 1992

7 7.1 TOTAL NUMBER OF PAGES 38

7.2 NUMBER OF REFERENCES 14

8 8.1 CORPORATE AUTHOR (S)

Surveillance Research Laboratory

8.2 DOCUMENT SERIES and NUMBER

Technical Report 0096

9 REFERENCE NUMBERS

a. Task :

b. Sponsoring Agency :

10 COST CODE

11 IMPRINT (Publishing organisation)

Defence Science and Technology Organisation

12 COMPUTER PROGRAM (S) (Title (s) and language (s))

13 RELEASE LIMITATIONS (of the document)

Approved for Public Release.

Security classification of this page : UNCLASSIFIED

14 ANNOUNCEMENT LIMITATIONS (of the information on these pages)

No Limitation

15 DESCRIPTORS		**16** COSATI CODES
a. EJC Thesaurus Terms	Algorithms Antenna arrays Jamming Noise Phased arrays	170403
b. Non - Thesaurus Terms	Adaptive sidelobe cancellation	

17 SUMMARY OR ABSTRACT
(if this is security classified, the announcement of this report will be similarly classified)

(U) This report assesses the performance of an adaptive sidelobe cancellation system based on the Modified Gram-Schmidt algorithm. A large phased array antenna has been modelled utilising this adaptive sidelobe cancellation technique and relevant scenarios simulated. In order to reduce antenna pattern degradation, noise injection has also been implemented.